Lawrence Berkeley Laboratory

UNIVERSITY OF CALIFORNIA

ENERGY & ENVIRONMENT DIVISION

Presented at the American Section/International Solar Energy Society Solar Jubliee, Phoenix, AZ, June 2-6, 1980

NATURAL CONVECTION IN ROOM GEOMETRIES

Ashok Gadgil, Fred Bauman, Ronald Kammerud, and Kalev Ruberg

June 1980

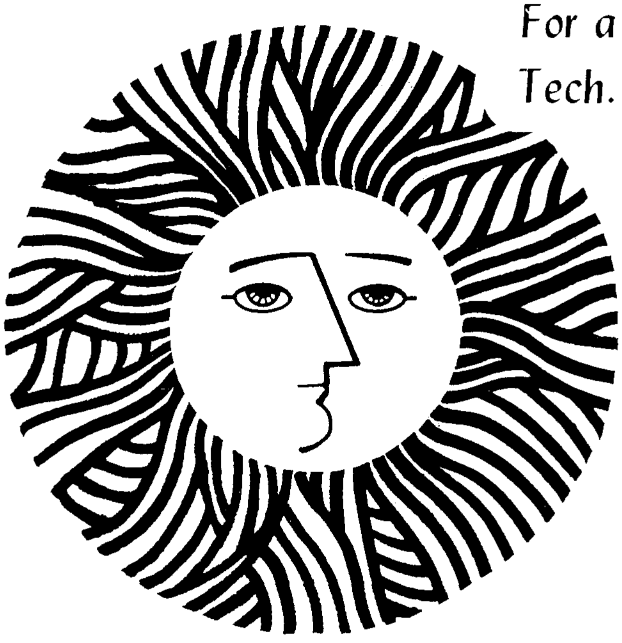

Prepared for the U.S. Department of Energy under Contract W-7405-ENG-48

LBL 9297
June 1980

NATURAL CONVECTION IN ROOM GEOMETRIES*

Ashok Gadgil, Fred Bauman, and Ronald Kammerud
Passive Solar Analysis and Design Group
Lawrence Berkeley Laboratory
University of California
Berkeley, CA 94720

Kalev Ruberg
National Bureau of Standards
Gaithersberg, Maryland 20760

ABSTRACT

Computer programs have been developed to numerically simulate natural convection in room geometries in two and three dimensions. The programs have been validated using published data from the literature, results from a full-scale experiment performed at Massachusetts Institute of Technology, and results from a small-scale experiment reported here. One of the computer programs has been used to study the influence of natural convection on the thermal performance of a single thermal zone in a direct-gain passive solar building. The results indicate that the building heating loads calculated by standard building energy analysis methods may be in error by as much as 50% as a result of their use of common assumptions regarding the convection processes which occur in an enclosure. It is also found that the convective heat transfer coefficients between the air and the enclosure surfaces can be substantially different from the values assumed in the standard building energy analysis methods, and can exhibit significant variations across a given surface.

1. INTRODUCTION

In spite of the fundamental role played by natural convection in both conventional buildings and passive solar systems, it has received relatively little experimental or analytic attention within the building sciences. Within a single thermal zone, natural convection and thermal radiation are jointly responsible for the distribution of heat from collection and/or storage media to the building occupants, the occupied space, or to non-illuminated storage materials. In the multi-zone configurations characteristic of most occupied buildings, convection processes contribute to the thermal transfers between zones. Buoyancy-driven convection is responsible for stack effect cooling in sunspaces, multi-story atria, and in other thermal chimney designs; and finally, many passive solar concepts such as double envelope structures, thermocirculation systems, and other air collector systems rely almost exclusively natural convection for their operation. Recent research results have emphasized the importance of natural convection processes. Analyses performed by the Los Alamos Scientific Laboratory on the Douglas Balcomb house [1] have implied the dominance of convective coupling of thermal zones in an occupied structure. Preliminary results from the work described herein [2] indicate that significant variations in the nature of the convective heat transfer processes can occur in physically similar, and common, direct solar gain designs.

The work reported here consists of:

(1) The development and validation of a numerical analysis technique for studying convective heat transfer in buildings.

(2) The use of this analysis technique to study the quantitative role of natural convection in the thermal performance of a direct solar gain structure, and thereby to examine the accuracy of standard assumptions regarding convective heat transfer within a zone in a building.

2. PROBLEM DEFINITION

In the published literature, the problem of natural convective heat transfer in an enclo-

*This work was supported by the Research and Development Branch, Passive and Hybrid Division, of the Office of Solar Applications for Buildings, U.S. Department of Energy, under Contract No. W-7405-ENG-48.

sure is typically simplified to the configuration illustrated in Fig. 1. In a two-dimensional rectangular enclosure, one vertical surface is maintained at a constant temperature T_H, and the opposite vertical surface is maintained at a lower constant temperature T_C. The horizontal surfaces are adiabatic (perfectly insulated). This was one of the configurations chosen for the numerical and experimental studies for comparisons with published data.

In the configuration illustrated in Fig. 1, variations in density drive the enclosed fluid up the heated wall, along the top horizontal surface, down the cooled wall, and along the bottom horizontal surface, completing the convective loop. Characteristics of the flow such as the mean air temperature, convection coefficients between air and walls, flow velocities, etc. are completely determined by specification of the three independent dimensionless parameters listed below:

(1) Aspect ratio: $A = H/L$ where H = enclosure height and L = enclosure length.

(2) Prandtl number: $Pr = \nu/\alpha$ where ν = kinematic viscosity and α = thermal diffusivity.

(3) Raleigh Number: $Ra_L = Gr_L Pr = g\beta\Delta T L^3 Pr/\nu^2$, where Gr_L = Grashof number, g = acceleration due to gravity, β = coefficient of thermal expansion, and ΔT = characteristic temperature difference = $T_H - T_C$.

These parameters include all of the relevant information regarding the enclosure geometry, the fluid properties, and the relative strength of buoyancy and viscous forces, respectively. For a rectangular room twice as long (5.5 m) as it is high (2.75 m) filled with air at 21°C and with at least a 1°C temperature difference between vertical walls, these parameters take the values:

$$A = 0.5,$$

$$Pr = 0.71, \text{ and}$$

$$Ra_L \geq 1 \times 10^{10}.$$

Heat input or extraction through one vertical surface on an enclosure is a reasonable model for many situations arising in buildings; for example, it may represent heat gain from an unvented Trombe wall, or heat loss through windows in single and multi-story buildings. In addition, a previous study [3] indicates that in warm climates the heat losses through the walls and windows (the vertical surfaces) are larger than the losses through the floor and the ceiling (horizontal surfaces) in a well-insulated, single story, residential building. However, it has been shown [2] that convective heat transfer processes are highly dependent on the design details of the structure being studied (e.g. [2]) and the range of thermal boundary conditions that might be encountered in the structure. An unmanageably large number of experiments would be required to thoroughly explore natural convection phenomena in buildings empirically. The present study circumvents this difficulty by focusing on the development of a general computerized numerical method for analysis of natural convection, and on the validation of the method using results from a few selected experiments. The computer code can then be applied to a broad range of studies of natural convection in buildings.

3. ANALYSIS DESCRIPTION AND COMPARISON WITH PUBLISHED DATA AT LOW RAYLEIGH NUMBERS

Little numerical work has been published on natural/buoyant convection at Rayleigh numbers in excess of 10^7. In this flow regime fluid velocities become relatively large. If the popular Central Difference Scheme (CDS) is used for casting the equations governing the fluid flow into finite difference form, the large velocities necessitate an impracticably fine mesh size to ensure numerical stability of the solution procedure (e.g. [4]).

In recent years Spalding [5] has proposed a differencing scheme that overcomes this difficulty; it allows relatively coarse grid spacings without seriously compromising accuracy and solution stability [6]. Two computer programs (CONVEC2 and CONVEC3) were developed based on this differencing scheme. These programs respectively solve the coupled two- and three-dimensional conservation equations with the Boussinesq approximation:

Continuity:

$$\mathrm{div}(\vec{V}) = 0$$

Momentum:

$$\hat{Re}\,\frac{d\vec{V}}{dt} + (\vec{V} \cdot \vec{\nabla})\vec{V} = \nabla^2\vec{V} - \mathrm{grad}\ p + Gr\theta\delta_i^3$$

Energy:

$$Re\,\frac{\partial\theta}{\partial t} + (\vec{V} \cdot \mathrm{grad})\theta = \frac{1}{Pr}\nabla^2\theta$$

These computer programs can be applied to fluid flow problems driven by predefined temperature distributions on the enclosure surfaces and/or by pressure differentials between specified locations on the boundary. To date, a turbulence model has not been incorporated into either computer program, so the analyses are limited to steady (laminar) flows. (For a more detailed description of the analysis technique, see [7] and references cited therein.)

Validation of the two computer programs CONVEC2 and CONVEC3 has been undertaken by comparing the calculated results to various published numerical and experimental efforts and by comparison to two recent experiments utilizing room geometries. The comparison to the low Rayleigh number data cited in the literature is described below; validations at the higher Rayleigh numbers characteristic of buildings are described in the next sections.

It is noted that the mesh sizes used in all validations were relatively coarse (the finest two-dimensional mesh size was 17x20). The grid lines were distributed evenly throughout the interior of the fluid volume with a concentration of grid lines near the enclosure boundaries; this permitted simulation of the sharp changes in flow properties associated with a developed boundary layer. Sensitivity analyses indicated that it was adequate to position three grid lines parallel and adjacent to each enclosure surface for this purpose.

A quantity of particular importance in the problem defined by Fig. 1 is the magnitude of convective heat transfer, measured by the Nusselt number. For a square enclosure (H = L in Fig. 1), the average Nusselt number can be defined as:

$$\overline{Nu}_L = \frac{1}{T_H - T_C} \int_0^1 \frac{\partial T}{\partial y}\, dx$$

In Fig. 2, Nu_L calculated with the convection code is plotted as a function of Rayleigh number. On the same graph, relevant numerical and experimental results for $10^4 \leq Ra_L \leq 10^9$ from various investigators have been superimposed; as shown, the agreement is quantitatively acceptable.

4. EXPERIMENTS AND ANALYSIS VALIDATION AT HIGH RAYLEIGH NUMBERS

Existing experimental data has been limited to Rayleigh numbers of less than 10^9--at least an order of magnitude below that which characterizes full-scale building geometries. In addition, most of the data is for large aspect ratios, typifying fluid flow in narrow vertical channels. Two recent experiments ([2], [8]) have expanded the data base into the geometric and kinematic region of interest to the buildings sciences. The experiments are described below and their results are compared to the predictions of the convection analysis code.

A. Small-Scale Experiment

A small-scale experiment, coordinated with the analysis, is being carried out at Lawrence Berkeley Laboratory. The results from the first phase of this experiment are reported below.

A schematic cross-sectional view of the experimental configuration is shown in Fig. 3; the apparatus had inside dimensions of 12.7 cm high by 25.4 cm long and a horizontal extent of 76.2 cm to minimize three-dimensional effects. Water was used as the working fluid; this allowed representative Rayleigh number values to be obtained in a small-scale apparatus. The range of parameters covered by this experiment are:

$$A = 0.5$$

$$2.6 \leq Pr \leq 6.8$$

$$1.6 \times 10^9 \leq Ra_L < 5.4 \times 10^{10}$$

The opacity of water to thermal radiation implies that the experiment was not a direct, scaled approximation to a real room--the experiment allowed measurement of the purely convective part of the heat transfer process being studied* and from this standpoint, was ideal for validation of the convection analysis code.

In experimental modeling of convective heat transfer processes, the behavior of a fluid with Prandtl number less than 1.0 cannot be accurately simulated with a working fluid having a Prandtl number much greater than 1.0 [9]. Therefore, the magnitude of the Nusselt number measured in this experiment is not accurate for an air-filled enclosure. However, the general fluid behavior and parametric relationship observed in the experiment can be expected to be representative of an air-filled cavity.

The heat transfer data obtained from the experiment are presented in the form of $\mathrm{Log}_{10}(Nu_{L_{IN}})$ vs. $\mathrm{Log}_{10}(Ra_L)$ in Fig. 4. In this figure, $Nu_{L_{IN}}$ (Nusselt number) is a measure of the strength of the convective heat transfer at the heated wall. On the same figure, experimental results from a study by MacGregor and Emery [9], and predictions from an analytic study by Raithby et al. [10] are shown; the present experiment is in quantitatively good agreement with both of these previous results. (Note that at the high Rayleigh numbers shown in the figure, the Nusselt number is relatively insensitive to the aspect ratio; [11, 12].

*The maximum contribution of thermal radiation to the measured Nusselt number was calculated to be less than 2%.

In order to use the data from this experiment for validation of the two-dimensional convection code, the computer program was modified to incorporate the temperature dependence of the physical properties of water. Sensitivity studies using the computer program demonstrated an increase of up to 10% in the Nusselt numbers when the properties were allowed to vary with temperature rather than being fixed at their average values. Due to lack of sufficiently detailed experimental instrumentation, best estimates of some enclosure surface temperature profiles were necessary to complete the input to the analysis program. These surface temperature estimates are believed to have errors of less than $\pm 10\%$. To date, the sensitivity of the prediction of the computer code to these uncertainties has not been thoroughly investigated.

Comparisons of the predictions of the computer code with the experimental results for the extent of stratification in the core region are shown in Figs. 5 and 6. These figures show the temperature profiles along vertical and horizontal lines through the geometric center of the enclosure for $Ra_L = 2.4 \times 10^9$ and $Ra_L = 4.7 \times 10^{10}$, respectively. The excellent agreement of the numerical prediction of the temperature profiles in the central core at the lower Rayleigh number (Fig. 5) indicates that the program is addressing the fundamental characteristics of the flow succesfully at this Rayleigh number (2.4×10^9). The numerically predicted vertical centerline temperature profile at the higher Rayleigh number (4.7×10^{10}, Fig. 6) exhibits a shift to smaller temperature gradients in the central core region associated with an increased gradient near the horizontal surfaces. There are three likely candidates for the source of this discrepancy: (1) The potential for transitional flow (between steady laminar and fully turbulent) at this value of Ra_L could contribute to the noted differences between experiments and numerical results; (2) Due to increased convective effects at this higher Ra the errors in the estimates of surface temperatures immediately upstream from the centerline region may have a significant effect on the magnitude of the calculated temperature profile at the centerline; (3) The coarse mesh size used in the present numerical studies may also have been a contributing factor to the disagreement at this high value of Ra_L. Ongoing work is expected to shed light on this question; until the source of the discrepancy is understood, however, the comparison of stratification profiles implies that the convection code properly represents the fundamental character of the flow for the smaller value of Ra_L and is qualitatively correct for all $Ra_L < 5 \times 10^{10}$.

The Nusselt number predictions made by the computer code are compared to the corresponding measurements in Table 1; the surface temperature distributions used in the simulations are also indicated in this table. The two separate numerical simulations (Runs 2a and 2b) made at the higher Rayleigh number give an indication of the sensitivity of the predicted Nusselt number to differences in the details of a surface temperature specification.

B. Full-Scale Experiment

Natural convection was investigated in a full-sized test room measuring 3.6 m wide by 3.6 m long by 2.0 m high. A schematic of the experiment is shown in Fig. 7. Heat was supplied to the test room by an electric resistance heating plate on the floor. A single-pane window was located on one wall of the enclosure. Though the window represents only 2% of the envelope area of the test room, it dominated the thermal load; 22% of the total losses from the structure were measured to be through this surface. Steady-state conditions were maintained by controlling the temperature of the air outside the test room to within $\pm 0.2^{o}C$ of its average value. The construction was sufficiently airtight that the effects of infiltration could be ignored.

The heater plate configuration was intended to represent the solar irradiated area of the floor; its rectangular shape and its size (1.16 m^2) were well-matched to those of the 1.12 m^2 window, and its heating capacity (448 W/m^2) was selected to approximate solar radiation falling on a dark-colored floor with low thermal capacity at noon on a clear day at $40^{o}N$ latitude. The parameters for this experiment were:

$$A = 0.58$$

$$Pr = 0.71$$

$$Ra_L = 5 \times 10^{10}$$

Experimental measurements were performed in a vertical plane (AA in Fig. 6) perpendicularly bisecting the window surface. Four types of data were collected inside the test room:

- Air Temperature: A vertical array of eleven thermistors was mounted on a motorized boom which traversed the test room in the measurement plane. The array has 20 cm vertical spacings in the center and 10 cm spacings near the ceiling and floor; data were recorded at 20 cm horizontal intervals as the boom moved across the room. This resulted in a grid of 11x18 temperature data points in the measurement plane.

- Surface Temperatures: The surface temperatures of the heater plate, both sides of the window, and the wall opposite the window were measured and recorded.

- Air Velocity: Local air velocities in the horizontal and vertical directions were measured using a single direction hot-wire anemometer. Data were collected at 24 cm horizontal intervals at four different heights above the floor. In addition, air velocities were manually measured by timing the traversal of suspended particles over a known path length.

- Air Current Visualization: Kerosene vapor was introduced into the test room and illuminated by a vertical plane of light. The light source and vertical baffles were located outside the room; the light was projected through the window and the vapor particle distribution was video-recorded through a viewing port.

Convection observed in the test room was characteristic of the transition regime, between laminar and turbulent flow. The air flow was periodic and consisted of three distinct phases:

(1) A calm phase, lasting about 1 minute, characterized by laminar flow of air over the heater plate in a "wave" configuration. Upon reaching the rear wall, the direction of flow became vertical.

(2) An acceleration phase, lasting approximately 20 seconds. This period was characterized by an erratic increase in air flow velocity.

(3) A high velocity phase. This phase lasted about 5 seconds; it was characterized by a fluctuating air velocity, with a main plume rising 0.6 m from the rear wall. Simultaneously, cold air was entrained into a layer formed over the heater plate. The cool air began to increase in temperature and the entire cycle was repeated.

The highest observed air velocities, 112 cm/sec, coincided with the plume eruption. The vertical plume velocity, as shown in the velocity profiles in Fig. 8a, slowed to 4 cm/sec upon changing direction and dispersing at the ceiling. The horizontal flow is illustrated in Fig. 8b. The periodic character of the flow was evident at the ceiling. This flow along the ceiling fed the laminar downdraft at the window, so the periodicity was not evident in the cold air flow across the floor, towards the heater plate. Both horizontal layers, at the floor and ceiling, were 20-25 cm thick, leaving a large stagnant volume in the center of the room.

Temperature measurements were converted to isotherms separated by intervals of 5% of the maximum surface temperature difference in the room. The isotherms were referenced to the mean temperature of the room, indicated on Fig. 9 as 0.00. From the isotherms, the air flow patterns described above may be discerned: the plume over the heater plate, a layer of warm air at the ceiling, a cool air current at the window and along the floor, and a somewhat isothermal area in the center of the room. For more details of this experiment, see Ref. [8].

Data from this full-scale experiment was compared with the predictions from the three-dimensional version of the numerical code. The surface temperature profiles used in the analysis were estimated from the available data using a thermal balance technique. It is noted that the effects of radiation on the temperature probes are expected to bias the measured air temperatures towards higher values by an unknown amount. This effect was not accounted for in the thermal balance. This bias also affects the comparisons between the isotherms predicted by the numerical scheme (Fig. 10) and the experimental results (Fig. 9). In light of these limitations, the agreement is satisfactory.

An energy balance calculation to estimate the convective heat flux from the hot plate in the experiment yields a value of 85 W/m^2. The computer program predicts a convective heat flux from the hot plate of 56 W/m^2.

Since the flow is in the transition regime, use of a model for buoyancy-induced turbulent flow would be expected to improve the agreement.

5. NATURAL CONVECTION IN BUILDING ENERGY ANALYSIS

While most computerized building energy analysis computer codes (BLAST,* DOE-2,+ etc.) and other passive solar system analysis programs assume constant convective heat transfer coefficients for the surfaces of the building being analyzed,† it has been shown (2) that the coefficients are actually very

*BLAST (Building Loads Analysis and System Thermodynamics) is copyrighted by the Construction Engineering Research Laboratory, U.S. Dept. of the Army, Champaign, Illinois.

+DOE-2 is a public domain program being developed by the Division of Communities and Building Energy Systems, Department of Energy.

†Some of the codes do utilize convection coefficients for non-vertical surfaces which are sensitive to the direction of heat flow, but not to the magnitude of the temperature difference between the room air and surface or to the possibly large effects induced by the differences in surface temperatures.

sensitive to the detailed temperature distributions on those surfaces. In order to assess the effects of this simplification of the accuracy of results from these programs, the convection code was used iteratively with BLAST to obtain self-consistent surface temperature distributions and convection coefficients.

A south facing zone of a multizone building was studied. This zone had dimensions of 3.66 m wide x 9.14 m high. The interior of the anlayzed zone was made up of 14 surface segments. The two "end surfaces" (the east partition wall and the west exterior wall) measured 2.44 m x 3.66 m and were very highly insulated. The other four major surfaces (ceiling, floor, gypboard north partition wall, and the south exterior wall) were each divided into three equal subsurfaces; The individual subsurface extended the full 9.15 m length of the zone. The middle section of the south wall was specified as double pane window. The iterative analysis was performed for the nighttime period when this direct-gain space was in a loss mode.

Due to the surface temperatures and the zone geometry, the convective flow was expected to be two-dimensional in character. The two-dimensional convection code was used to simulate the details of the convection process in that zone and used to calculate convection heat transfer coefficients for each subsurface. These coefficients were used as input to BLAST, which then was used to calculate the resulting surface temperatures. These temperatures were used as input to the convection code and the entire procedure was iterated to convergence.

BLAST performs a full thermal balance on all surfaces of the zone under study. The thermal balance accounts for thermal radiation between zone surfaces, convection between zone air and each surface, and conduction through each surface. For simplicity, the external weather was chosen to produce effectively steady-state conditions. The output of BLAST includes zone loads, air and mean radiant temperatures, and the surface temperatures and heat fluxes at each surface of the zone.

The convection analysis code calculated local air temperatures at each node, but did not include source terms; the average air temperature that was calculated from the node temperatures represented the balance point for the zone under the given surface temperature distributions. For this reason, the BLAST simulation from which the surface temperatures were taken did not include auxiliary heating and/or cooling of the zone in which the convection was to be analyzed.

The results of the analysis are shown in Table 2. Surfaces are numbered sequentially around the zone; results for the thermal parameters for each subsurface of the primary zone surfaces appear in the table. Case I refers to standard assumptions and case II refers to the values after the iterations.

The convective coefficients are seen to change substantially from their standard assumed values for most of the surfaces. However, this has a smaller effect than expected on the thermal behavior of the zone for the following reasons:

(1) The surfaces which are coupled more strongly to the room air through larger convective coefficients in case II have smaller resulting temperature deviations from the room air temperature than in case I; this has a moderating influence on what otherwise would have been a larger convective (and radiative) heat flux. On the other hand, the surfaces which are coupled less strongly to the room air through smaller convective coefficients in case II tend to have larger resulting temperature differences from the room air than in case I; this increases what otherwise would have been a smaller convective (and radiative) heat flux.

(2) In addition to convection, radiative exchange is equally important in thermally coupling the zone surfaces to one another and is independent of the magnitude of the convective coefficients (to the first approximation). For this reason, changes in the convective coefficients will have a smaller percentage effect on the total heat flux (convection + radiation) from a surface.

The net result of these two factors is that the average air temperature and the mean radiant temperature of the zone have remained practically unchanged after the iterative procedure between BLAST and the convective code was completed.

The convective heat flux from the warm north wall shows a significant variation along its height (15.4 W/m^2 from the bottom of the wall to 7.2 W/m^2 from the top). As cold air warms up at the bottom of the north wall and rises, the upper portions of the wall encounter relatively warmer air and can contribute relatively less heat to this air. If this north wall were an (indirect) heat storage system, the convective recovery of heat from the bottom portions of the wall would be nearly twice as rapid as that from the top portions, in this configuration. Another interesting feature is the very large convective coefficient (8.9 W/m^2 ^{o}C) for the portion of the cool ceiling directly warmed by the updraft from the warm north wall. Since the ceiling was well insulated, the temperature difference between this portion of the ceiling and the room air was decreased (by about 50%) with only a negligible change in the heat loss to the attic.

The portion of the south wall directly below the double-pane window encounters a downdraft of cold air that has lost heat through the window. This downdraft of air is actually colder than the interior surface of the bottom portion of the south wall (this surface is warmed by radiative exchange with the north wall). Thus, although the bottom section of the south wall is actually cooler than the average room temperature, it deposits heat into the cold downdraft flowing across it. This has resulted in its convective coefficient being negative (the convective coefficients are defined with respect to average room air temperature).

The convection code predicts a vertical stratification in the bulk of room air of no greater than 0.7 ^{o}C/m at the center of the zone.

6. SUMMARY

A numerical technique for modeling natural convection in room geometries has been developed. The numerical predictions from this technique have been compared with various published data and demonstrate satisfactory agreement. The results from a small-scale and a full-scale experiment studying natural convection in room geometries have been presented. Comparisons of the numerical predictions with the results of these experiments exhibit satisfactory agreement. The convection code has been used in conjunction with the BLAST computer program to investigate the thermal behavior of a realistic direct-gain zone configuration in the loss mode. The results indicate that:

- The detailed modeling of convection may have a small effect on the zone air temperature and the mean radiant temperature in the loss mode.
- Some of the convective coefficients can be substantially different from the values assumed by the standard building energy analysis methods.
- The convective coefficients can show a significant variation across a given zone surface.
- Such variations in convective coefficients could have a substantial effect on the distribution of gains and losses from various surfaces in a passive solar room configuration.

7. REFERENCES

(1) Balcomb, J.D., Hedstrom, J.C., and Moore, S.W., Los Alamos Scientific Lab Report No. La-UR-79-2659 (1979).

(2) Bauman, F., Gadgil, A. Kammerud, R., and Greif, R., Paper No. ASME 80-HT-66 in Proceedings, 19th National Heat Transfer Conf., 27-30 July 1980, Orlando, Fla. (Lawrence Berkeley Laboratory Report LBL-10257).

(3) Wall, L.W., Dey, T., Gadgil, A.J., Lilly A.B. and Rosenfeld, A.H., "Conservation Options in Residential Energy Use: Studies Using the Computer Program TWOZONE," Lawrence Berkeley Laboratory Report LBL-5271 (August 1977).

(4) Roache, P.J., Computational Fluid Dynamics, Hermosa Publishers (1972).

(5) Spalding, D.B., "A Novel Finite Difference Formulation for Differential Expressions Involving Both First and Second Derivatives," Int'l J. Numerical Methods in Engrg., 4, 551-559 (1973).

(6) Runchal, A.K., "Convergence and Accuracy of Three Finite Difference Schemes for a Two-Dimensional Conduction and Convection Problem," Int'l J. Numerical Methods Engrg., 4, 541-550 (1973).

(7) Gadgil, A., Ph.D. Thesis, "On Convective Heat Transfer in Building Energy Analysis," Department of Physics, University of California, Berkeley (1980).

(8) Ruberg, K., Master's Thesis, "Heat Distribution of Natural Convection: A Modeling Procedure for Enclosed Spaces," Dept. of Architecture, Massachusetts Institute of Technology, Cambridge, MA. (1978).

(9) MacGregor, R.K. and Emery, A.F., "Free Convection Through Vertical Plane Layers--Moderate and High Prandtl Number Fluids," J. Heat Transfer, Trans. ASME, 91, 392-401 (1969).

(10) Raithby, G.D., Hollands, K.G.T., and Unny, T.E., "Analysis of Heat Transfer by Natural Convection Across Vertical Fluid Layers," J. Heat Transfer, Trans. ASME, 99, 287-293 (1977).

(11) El Sherbiny, S.M., Raithby, G.D., and Hollands, K.G.T., "Heat Transfer by Natural Convection Across Vertical and Inclined Air Layers," ASME Paper No. 80-HT-67, presented at the 19th National Heat Transfer Conf., 27-30 July 1980, Orlando, Fla.

(12) Shiralkar G., Gadgil A. and Tien, C.L., "High Rayleigh Number Convection in Shallow Enclosures with Different End Temperatures," submitted for publication to Int'l Journal of Heat and Mass Transfer, (July 1980).

(13) de Vahl Davis, G., "Laminar Natural Convection in an Enclosed Rectangular Cavity," Int'l J. Heat & Mass Transf., 11, 1675 (1968).

(14) Emery, A.F., "The Effect of a Magnetic Field Upon the Free Convection of a Conducting Fluid," J. Heat Transfer, Trans. ASME, 85, 2, 119-124 (1963).

(15) Portier, J.J. and Arnas, O.A., Heat Transfer and Turbulent Buoyant Convection, Vol. II, Hemisphere Publishing Corp., 1977, pp. 797-806.

(16) Burnay, G., Hannay, J., and Portier, J., Heat Transfer and Turbulent Buoyant Convection, Vol. II, Hemisphere Publishing Corp., 1977, pp. 807-811.

(17) Rubel, A., and Landis, R., "Numerical Study of Natural Convection in a Vertical Rectangular Enclosure," Phys. Fluids Suppl. II., 12, II-208 (1969).

(18) Quon, Charles, "High Rayleigh Number Convection in an Enclosure: A Numerical Study," Phys. Fluids, 12, 1, 12-19 (1972).

(19) Fromm, J.E., "A Numerical Method for Computing the Nonlinear, Time Dependent, Buoyant Circulation of Air in Rooms," National Bureau of Standards Building Science Series, 39, 1971, pp. 451-464.

TABLE 1. COMPARISON OF HOT WALL $\overline{Nu}_{L_{IN}}$				
RUN	Ra_L	EXPT'L	NUMERICAL	SURFACE TEMPS FOR NUMERICAL SIMULATIONS
1	2.4×10^9	79 ± 6	105	ESTIMATED FROM EXP'T
2a	4.7×10^{10}	165 ± 12	168	ESTIMATED FROM EXP'T
2b			201	HOT & TOP WALL = T_H COLD & BOTTOM WALL = T_C

Table 2. Convective Analysis of a Single Zone, Gain Mode

SURFACE	SUBSURFACE NUMBER	SUBSURFACE LOCATION	STANDARD BUILDING ENERGY ANALYSIS ASSUMPTIONS: SURFACE TEMP °C	CONVECTION COEFFICIENT W/m²/°C	CONVECTIVE HEAT FLUX FROM ZONE TO SURFACE W/m²	TOTAL HEAT FLUX FROM ZONE TO SURFACE W/m²	VALUES AFTER ITERATION WITH CONVECTION CODE: SURFACE TEMP °C	CONVECTION COEFFICIENT W/m²/°C	CONVECTIVE HEAT FLUX FROM ZONE TO SURFACE W/m²	TOTAL HEAT FLUX FROM ZONE TO SURFACE W/m²
SOUTH EXTERIOR WALL	1	TOP	24.94	3.08	5.14	20.34	23.56	2.34	3.63	19.78
	2	MIDDLE/WINDOW	15.72	3.08	33.54	163.85	14.61	2.67	27.10	151.98
	3	BOTTOM	24.94	3.08	5.14	20.34	22.22	-2.64	-7.81	19.21
SLAB-ON-GRADE FLOOR	4	SOUTH	21.11	4.04	22.22	60.46	21.11	0.74	2.98	44.64
	5	MIDDLE	35.00	4.04	-33.89	-159.89	35.00	1.86	-18.30	-142.94
	6	NORTH	35.00	4.04	-33.89	-159.89	35.00	1.56	-15.40	-137.30
NORTH PARTITION WALL	7	BOTTOM	25.0	3.08	4.96	19.21	23.94	2.67	3.08	15.26
	8	MIDDLE	25.0	3.08	4.96	19.21	23.83	1.88	2.54	15.26
	9	TOP	25.0	3.08	4.96	19.21	23.89	2.38	2.98	15.26
CEILING TO ATTIC	10	NORTH	25.61	0.95	0.95	11.86	24.06	1.31	1.45	11.86
	11	MIDDLE	25.61	0.95	0.95	11.86	23.94	0.57	0.65	11.86
	12	SOUTH	25.61	0.95	0.95	11.86	23.94	0.60	0.69	11.86
			T_{AIR} = 26.61,		T_{MRT} = 25.91		T_{AIR} = 24.87,		T_{MRT} = 24.83	

Figure 1. Recirculating flow induced in a fluid inside a two-dimensional square cavity, defined by adiabatic floor and ceiling and isothermal walls, at temperatures T_H and T_C ($T_H > T_C$).

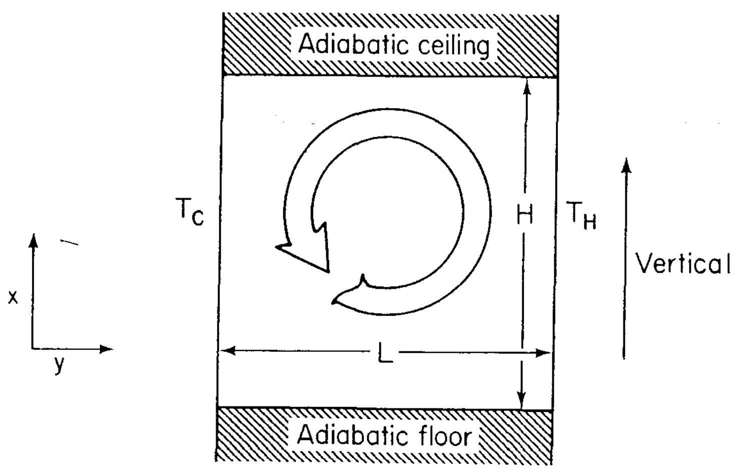

Figure 2. Dependence of $\overline{Nu}$ on Ra, for two-dimensional flow inside a square cavity; comparison with published results.

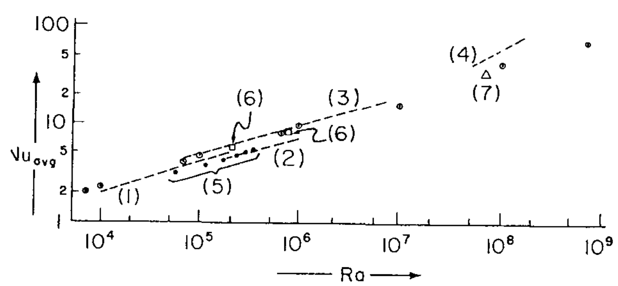

CURVE (1): DE VAL DAVIS CALCULATIONS
CURVE (2): FROM RESULTS OF EMERY, EXPERIMENTAL
CURVE (3): PORTIER ET AL., CALCULATIONS, Pr = 0.7
CURVE (4): BURNAY ET AL., DATA REDUCED FROM EXPERIMENTS, Pr = 0.7
RESULTS (5) ARE OF RUBEL AND LANDIS, CALCULATIONS
RESULTS (6) ARE FROM QUON, CALCULATIONS
RESULT (7) IS FROM FROMM
POINTS INDICATED BY ⊙ ARE FROM PRESENT CALCULATIONS

(1) - 1/2" Plexiglas
(2) - 3/16" Copper Sheet
(3) - Water
(4) - Thermofoil heaters
(5) - 3/8" O.D. copper tubing containing cooling water
(6) - High conductivity cement
(7) - 1/4" Plexiglas partition
(8) - Adjustable rod
(9) - 2" Polystyrofoam insulation board
(10) - Inside surface of polystyrofoam lined with polyethylene sheeting
(11) - Airspace
(12) - Thermocouple probe
(13) - Central Thermocouple array
(14) - Fiberglas insulation (2-layers)
(15) - Wood base

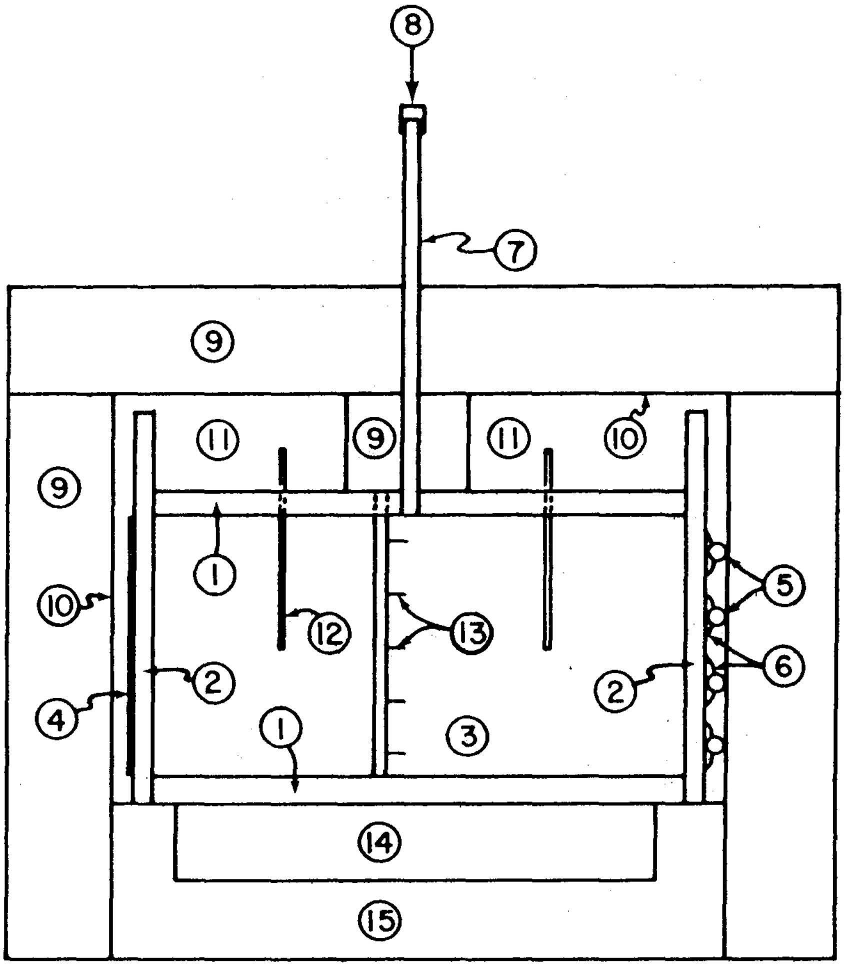

Figure 3. Apparatus Cross-Section

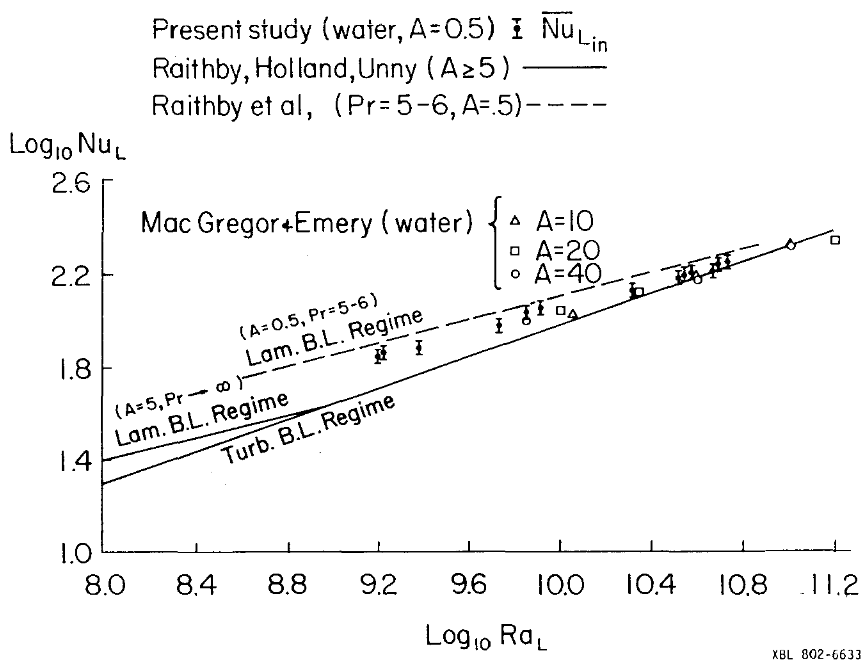

Figure 4. Heat transfer results and comparison

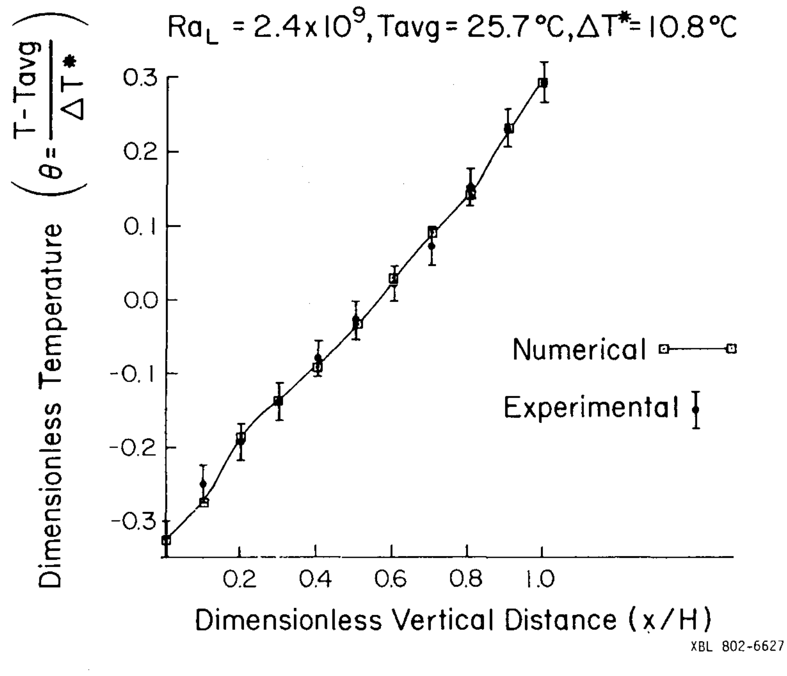

Figure 5. Vertical centerline (y/L=0.5) temperature profile

Figure 6. Vertical centerline (y/L=0.5) temperature profile

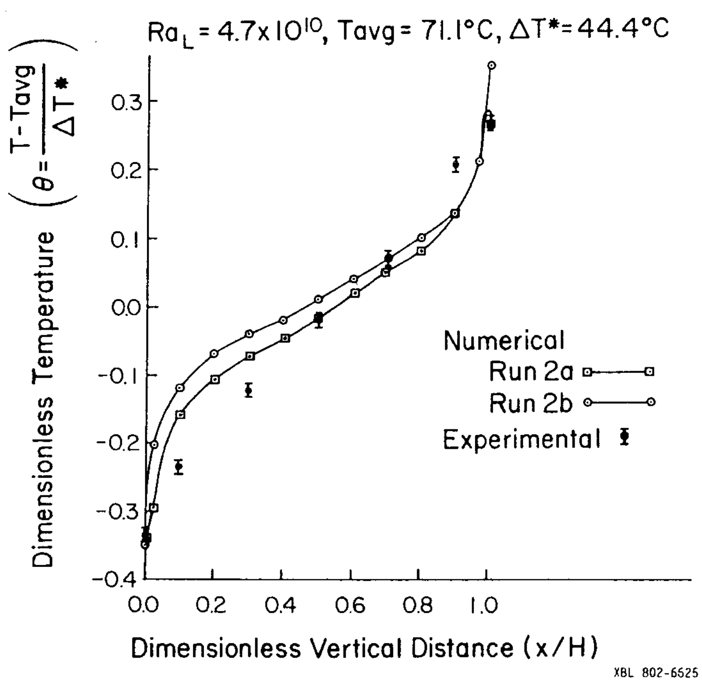

Figure 7. Schematic diagram of Ruberg's full-scale test

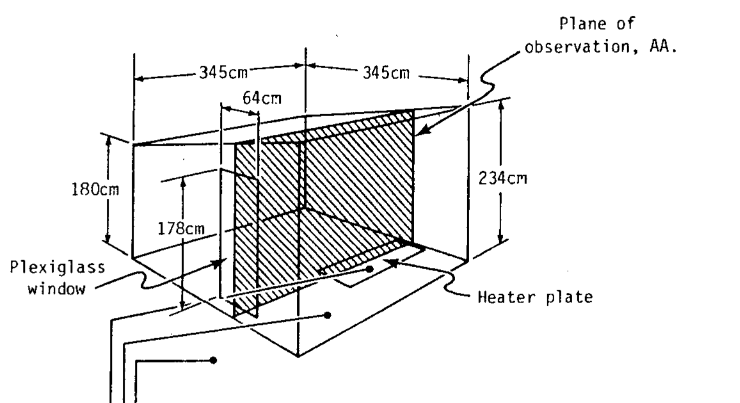

POSITION	C°	F°
Ambient air temperature	21.4	70.5
Room air temperature	40.6	105.1
Heater plate temperature	64.7	148.5

XBL7911-13133A

Figure 8a. Vertical Air Velocity Profile

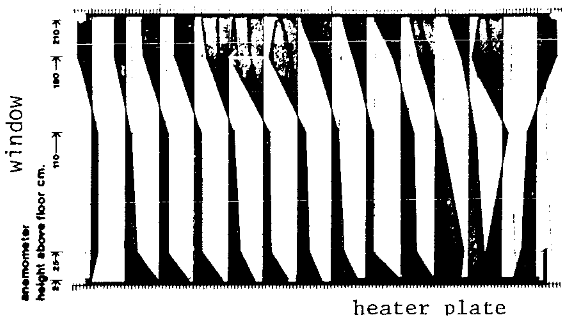

Figure 8b. Horizontal Air Velocity Profile

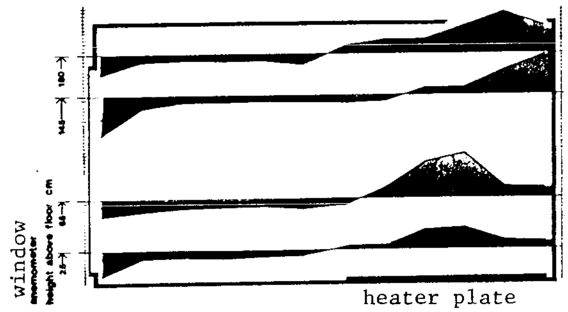

Figure 9. Isotherms in Full-Scale Experiment

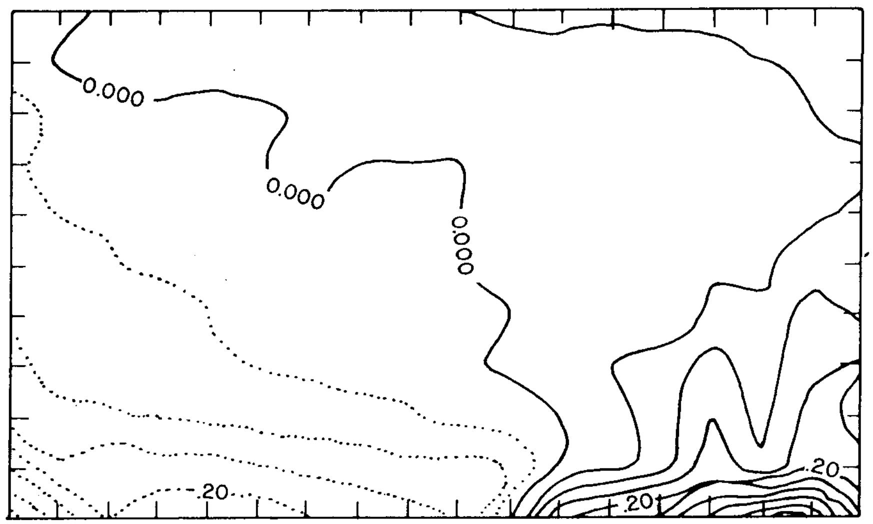

Figure 10. Numerically Predicted Isotherms for Full-Scale Experiment